Chapter 2
InP Ring-Shaped Quantum Dot Molecules by Droplet Epitaxy

Wipakorn Jevasuwan, Somchai Ratanathammapan, and Somsak Panyakeow

Abstract Droplet epitaxy technique is a key fabrication method to create ring-shaped nanostructures. InP ring-shaped quantum dot molecules are grown on In0.5Ga0.5P/GaAs(0 0 1) due to lattice mismatch of 3.8% between InP and In0.5Ga0.5P and isotropic migration property of In atoms during the crystallization step of In droplets on In0.5Ga0.5P. The ring shape, density of the ring and number of dots on the ring are controlled by various growth parameters such as deposition and crystallization temperatures, In deposition rate and thickness. InP ring-shaped quantum dot molecules provide photoluminescence peak at 740 nm (1.66 eV) with FWHM of 45 meV at 20 K. Potential applications of ring-shaped quantum dot molecules in quantum cellular automata are discussed.

2.1 Introduction

Quantum dot molecules (QDMs) are equivalent to artificial molecules while quantum dots (QDs) are considered as artificial atoms. QDMs hence possess more variety of properties and functionalities than a single quantum nanostructure like an individual quantum dot. Their fundamental characteristics and performances are based on how the QDMs are formed in terms of number of quantum dots in each QDM and in terms of their configurations and shapes of QDMs. QDMs are packages of QDs either in vertical or in lateral configuration. Multi-stacks of QDs with narrow spacers grown by residual strain of underneath QD layers are a typical vertical alignment of QDs in this type of QDMs [1]. Multi-stacked QDMs are key nanostructures for laser and solar cell applications [2–5] because of their high dot density and intermediate band formation due to uniform dot size. However,

W. Jevasuwan • S. Ratanathammapan • S. Panyakeow (✉)
Faculty of Engineering, The Semiconductor Device Research Laboratory, Electrical Engineering Department, Chulalongkorn University, Bangkok 10330, Thailand
e-mail: wipakornj@gmail.com; somchai.r@chula.ac.th; s_panyakeow@yahoo.com

J. Wu and Z.M. Wang (eds.), *Quantum Dot Molecules*, Lecture Notes in Nanoscale Science and Technology 14, DOI 10.1007/978-1-4614-8130-0_2,

lateral formation of QDMs gives more variety of geometrical configurations of QDMs depending on their number of QDs per QDM like bi-QDMs [6], quadra-QDMs [7], QDM chains [8] which have potential applications for single electron transistors, spintronics, quantum computation based on quantum cellular automata concept [9 12].

Beside the 0D quantum dot nanostructure, quantum ring (QR) is another feature which exhibits uniqueness due to 1D circular electron transport in ring-shaped nanostructure for magnetic sensitive behavior [13]. Most of the quantum rings are grown by droplet epitaxy magnetic sensitive behavior technique where group III elements like Ga, In in droplets are deposited and are followed by crystallization under pressure of group V elements like As, P [14–16]. During the crystallization process, the droplets will be transformed to ring shape due to out diffusion of group III elements from the center of the droplets because the crystallization is preferably started from the outer rim of the droplets. This technique has a growth merit that it can be conducted for either lattice-matched or lattice-mismatched system. GaAs single quantum rings and GaAs double quantum rings are examples of lattice-matched nanostructures grown by droplet epitaxy [17, 18]. InGaAs quantum rings grown on GaAs are realized from lattice-mismatched system [19, 20].

Combination of QDs and QRs in the same nanostructure is quite interesting due to dual characteristics of both 0D and 1D electron behaviors. Therefore, ring-shaped QDMs become our research target in this article. In order to do so, isotropic ring structure is required to create good ring-shaped QDMs. Isotropic out diffusion of group III elements during crystallization under the pressure of group V elements is a key selection of this ring-shaped QDMs where circular and uniform ring robe can be obtained. It is found that GaAs quantum rings and InGaAs quantum rings exhibit anisotropic property and show noncircular ring shape having difference ring robes along [110] and [1–10] crystallographic directions [21, 22].

InGaP having 0.5 In and 0.5 Ga compositions is lattice matched to GaAs [23]. Conventional growth technique of Stranski–Kastanov (S–K) is used to prepare InGaP buffer layer on GaAs substrate. InP quantum rings are then created on InGaP buffer layer by droplet epitaxy. Isotropic and circular quantum rings are obtained using InP/InGaP material system. Symmetrical and uniform ring robe of quantum rings is very important condition to further growth of ring-shaped QDMs. InP and InGaP have 3.8% lattice mismatching [24], and this condition can lead to the formation of QDs on the ring robe of QRs. Ring-shaped QDMs are then possible when the growth process continues. Control of some growth parameters such as droplet deposition temperature, crystallization temperature, and growth rate can define the number of QDs on the QRs. The dimension as well as the density of ring-shaped QDMs is also affected from those growth parameters. Experimental results will be discussed in the following section of the article.

InP is a direct band-gap semiconductor having good thermal, optical, and electrical properties for high performances of high power photonic and electronic devices [25]. InP nanostructure would further improve the device performances by the quantum effects like carrier and optical confinements. InP QDs as well as InP

ring-shaped QDMs can provide also narrow spectrum of red emission at 0.7 μm. Photoluminescence experiment of InP ring-shaped QDMs is also conducted and reported in this article.

2.2 The Formation Mechanism of InP Ring-Shaped QDMs

Semiconductor QDs are normally created by strain relaxation at the interface between lattice-mismatched semiconductor epitaxial layers such as InAs/GaAs. This growth technique is called Stranski–Krastanov (S–K) growth mode and is widely used in solid source molecular beam epitaxy (MBE) to prepare InAs QD nanostructure having good crystal quality for various nanoelectronic and nanophotonic applications.

This growth mechanism is self-assembly providing random individual InAs QDs spreading on the plane of epitaxial layer after the critical thickness of InAs wetting layer is reached (Fig. 2.1). InAs QDMs can be self-assembled by modification of growth process such as thin capping of initial InAs QDs leading to particular templates for InAs QDMs formation [26]. Partially capped InAs QDs can also provide QR templates for InAs bi-QDMs using gas source MBE [27]. The origin of InAs QDMs in these cases is based on elastic strain relaxation.

Droplet epitaxy is another alternative technique to prepare quantum nanostructures from both lattice-matched system such as GaAs on GaAs and small-lattice mismatched system such as InGaAs on GaAs. The growth process consists of two steps, i.e., droplet deposition and crystallization. The crystallization of the droplets begins at the outer edge of the droplets leading to the formation of QRs such as GaAs QRs and InGaAs QRs on GaAs substrates [28, 29]. Out diffusion of Ga and InGa atoms in the droplets under As pressure is the main growth mechanism of respective QRs (Fig. 2.2).

It is also found that there is some etching effect in the middle part of the Ga and InGa droplets in contact with the surface of GaAs buffer layer, which leads to deeper nanoholes inside the QRs. There will remain some residual strain field inside those deep nanoholes which originates InAs QD formation around and inside QRs [30, 31]. Anisotropy also occurs during InGaAs QR formation and gives birth to square-shaped nanoholes which also become templates for InAs quadra QDMs [7]. Combination of QR and QD formations in the same consecutive MBE growth

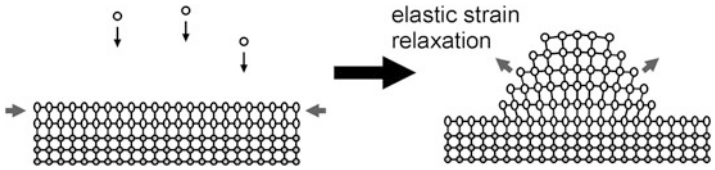

Fig. 2.1 Formation mechanism of self-assembled QDs by S–K growth mode

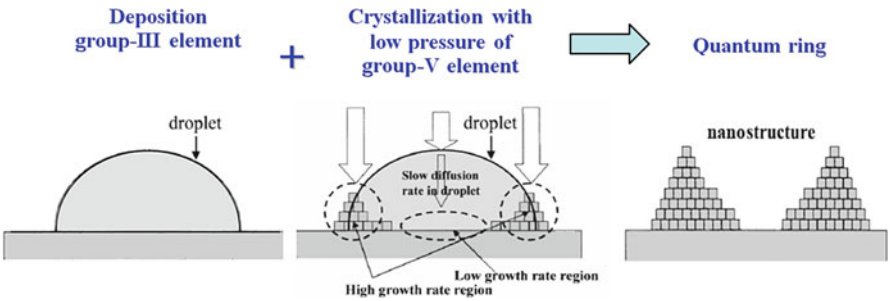

Fig. 2.2 Formation mechanism of self-assembled QRs by droplet epitaxy

process using both droplet epitaxy and strain relaxation would give more complex nanostructures of QDMs which are composed of both QD and QR at the same site.

In this article, we focus on the formation mechanism of InP ring-shaped QDMs which is quite different from the above-mentioned explanations in terms of both the material system and the outcome of combined QR/QD. In order to create InP quantum nanostructures, InGaP with In:Ga content of 50:50 layer is firstly prepared on GaAs substrate by conventional MBE growth method. This InGaP buffer layer is lattice matched to GaAs substrate; therefore, no strain exists in this bi-layer structure. Droplet epitaxy is applied for the whole process in creating InP ring-shaped QDMs. The very first step starts from In droplet deposition. Then, In droplets are exposed to P pressure at optimal crystallization temperature to form InP QRs. It is found that at small thickness of In droplets, only InP QRs are formed. These InP QRs have symmetrical circular shape due to isotropic crystallization in all crystallographic directions in the plane of growth. The ring robe of QR is uniform in terms of both width and height along the whole circumference of QR. When the thickness of In droplets becomes bigger, the InP QRs are transformed to InP ring-shaped QDMs during the crystallization process of those thick In droplets. The formation mechanism of InP QRs is similar to the explanation of InGaAs QRs. The only difference is their symmetrical circular shape of InP QRs compared to nonsymmetrical elliptical shape of InGaAs QRs. However, at thick In droplets, InP QRs are initially formed. The lattice mismatch between InP and InGaP is about 3.8%. This accumulates a strain in the InP QRs. When thickness of ring robe reaches a critical value, the same strain relaxation works and creates InP QD chain on the ring robe. The number of QDs on the ring robe depends on the droplet size which determines the dimension of ring diameter of InP ring-shaped QDMs. Smaller ring diameter has less number of QDs on the ring robe. The bigger ring diameter gives more QDs on the ring robe.

With single droplet epitaxy growth process, InP ring-shaped QDMs are created by the formation of QR as commonly being obtained in most of droplet epitaxy, and at the same time QDs are created on the ring robe by strain relaxation mechanism due to lattice mismatch between InP and InGaP epitaxial layers (Fig. 2.3).

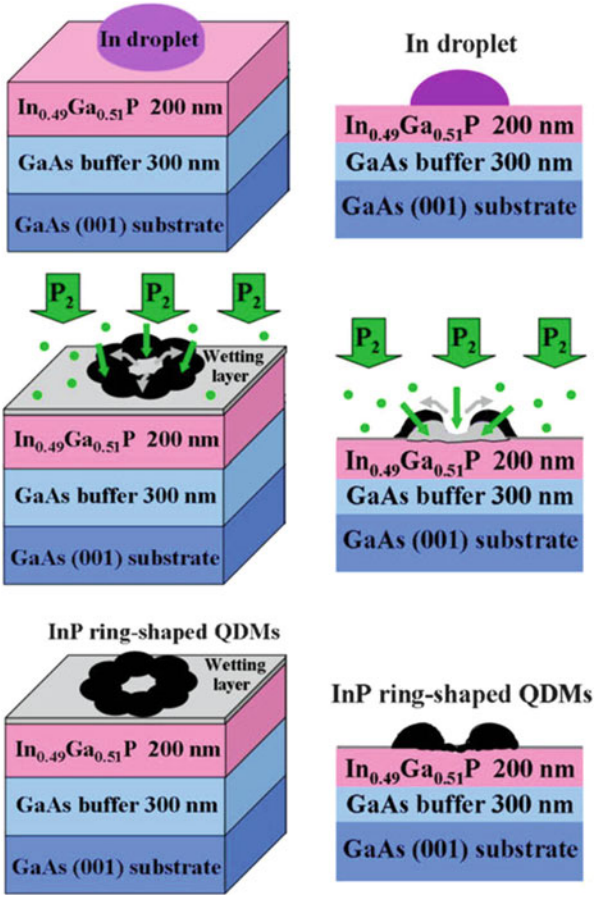

Fig. 2.3 Formation mechanism of InP ring-shaped QDMs by droplet epitaxy together with strain relaxation due to lattice mismatching of InP/InGaP

2.3 Experimental Works on Droplet Epitaxy of InP Ring-Shaped QDMs

InP ring-shaped QDMs are created by the droplet epitaxy technique. GaAs(0 0 1) substrate is used as the starting material. The GaAs wafer surface is cleaned by heating at 450°C for 1 h in the introduction chamber of MBE machine to eliminate the moisture. Then, the GaAs substrate is transferred to the growth chamber for surface oxide desorption under As pressure with BEP of 6×10^{-6} Torr at slow ramping of substrate temperature up to 610°C. After the oxide desorption process, GaAs surface becomes rough. It is necessary to grow 300 nm thick GaAs buffer layer on top to provide smooth GaAs surface for further MBE growth. Now, the

environment in the growth chamber is changed from As atmosphere to P atmosphere for the preparation of P-based materials. We choose In0.5Ga0.5P as buffer layer being grown on GaAs buffer layer. These two epitaxial layers are well lattice matched. A 200 nm thick In0.5Ga0.5P buffer layer is grown at 470°C with a BEP V/III ratio of 10 and with a growth rate of 0.5 ML/s. The formations of these bi-buffer layers (In0.5Ga0.5P/GaAs) are confirmed by the observation of 2×4 and 2×1 RHEED patterns, respectively.

Droplet epitaxy process starts when substrate temperature is decreased to 250°C without P beam to minimize the excess P on the surface. The background pressure in the growth chamber is kept at 10^{-9} Torr before indium droplet deposition begins. Indium droplets are spread on the InGaP surface at a deposition temperature between 120 and 290°C and a deposition rate from 0.2 to 1.6 ML/s. Indium thicknesses are varied from 1.6 to 6.4 ML. These variations of deposition parameters define the droplet size and droplet density which will be prime condition to control the configuration and number of dots in each InP ring-shaped QDMs.

Later on, P beam is introduced into the growth chamber again for crystallization process of InP nanostructures. The crystallization temperature is varied from 150 to 300°C under P BEP of 4×10^{-6} Torr for 5 min. At appropriate growth parameters, InP ring-shaped QDMs are formed.

InP nanostructures are then capped by 100 nm thick In0.5Ga0.5P double layers grown by the two-step technique. The first capping layer is 10 nm thick InGaP grown by migration enhanced epitaxy (MEE) at 300°C with 0.5 ML/cycle growth rate. The second layer of 90 nm thick InGaP is grown by the conventional MBE process at 470°C with the growth rate of 0.5 ML/s. This capped InP nanostructure sample is ready for ex situ photoluminescence measurement. The same growth process of InP ring-shaped QDMs is repeated on the top of sample surface with the same growth parameters to produce another layer of InP ring-shaped QDMs. Now, the sample surface morphology is ready to be observed by a tapping mode AFM. Fractional part of this sample is also the cross section observed by TEM to confirm the ring-shaped nanostructure. Schematic sample structures at different processing steps are displayed in Fig. 2.4.

Major characterization of InP ring-shaped QDMs is conducted by photoluminescence (PL) measurement. The PL intensity reflects the crystal quality of the nanostructures as well as their density. PL spectra give specific identity of the nanostructures as well as their uniformity. Ar+ laser with emission line of 478 nm is used to excite the sample. The excitation power is varied from 10 to 80 mW. The laser beam is chopped and focused onto the sample placed in a cryostat with a cooling sample temperature from room temperature down to 20 K. The PL signal is collected and resolved by a 1-m monochromator. The resolved PL signal is detected by a liquid nitrogen cooled InGaAs detector and sent to a lock-in amplifier for PL data analysis.

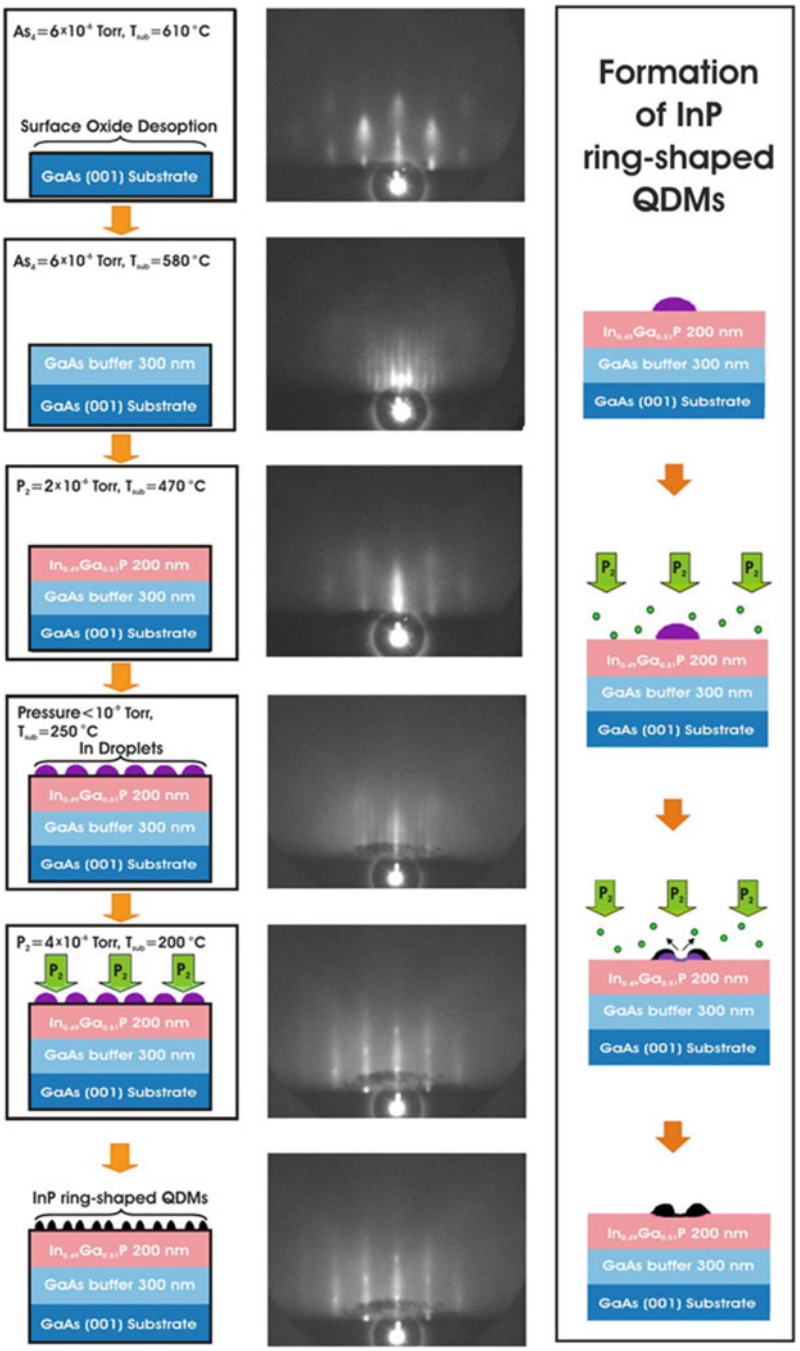

Fig. 2.4 Schematic diagrams of the sample structures grown at different steps and their in situ RHEED observations

2.4 Structural Evolution from In Droplets to InP Ring-Shaped QDMs

Indium droplets are starting elemental materials deposited on InGaP buffer layer at the beginning step of droplet epitaxy. Indium thickness (in ML), deposition rate (in ML/s), and deposition temperature (in °C) will define the droplet size and droplet density. The deposition temperature is a key parameter to control the droplet size and droplet density. At low deposition temperature, the droplet size is small but the droplet density is high. When the deposition temperature is higher, nearby small droplets will merge with each other resulting in a bigger droplet size, but the droplet density will become lower. The deposition rate will also affect the droplet evolution in a more complicated way. The indium thickness will keep the droplet density saturated with nominal droplet size.

When the crystallization of indium droplets is performed under P pressure, In droplets transform to InP QRs and InP ring-shaped QDMs, respectively. At small indium thickness, In droplets will be crystallized only to InP QRs as shown in Fig. 2.5. The ring has an isotropic shape and a small ring diameter. When indium thickness increases, InP QRs are transformed to InP ring-shaped QDMs as shown in Fig. 2.6. The ring diameter becomes longer with an increasing number of QDs and with a bigger dot size on the ring.

Figure 2.7 shows evolution from InP QRs to InP ring-shaped QDMs when indium thickness is varied from 1.6 to 6.4 ML (deposition temperature 250°C and crystallization temperature 200°C). Ring diameter, dot size, number of QDs per QDM, and density of ring-shaped QDMs are increased due to larger supply of

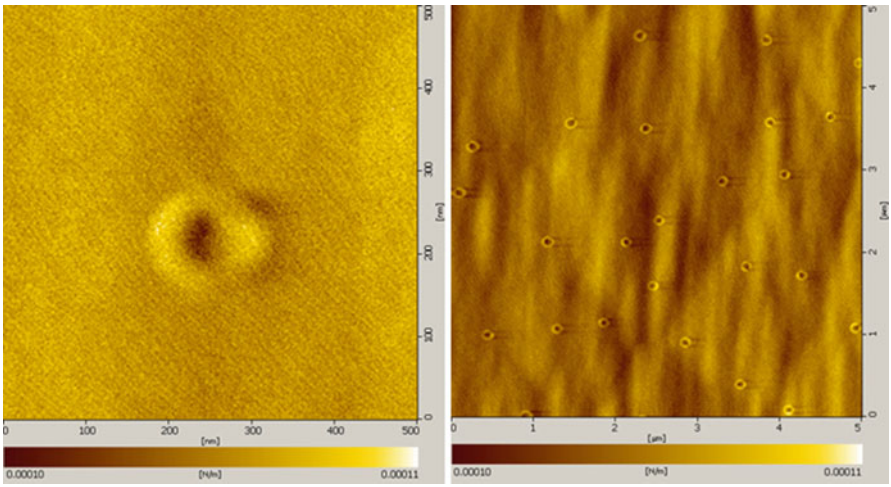

Fig. 2.5 AFM image of InP QRs grown from In thickness 1.6 ML (crystallization temperature 200°C)

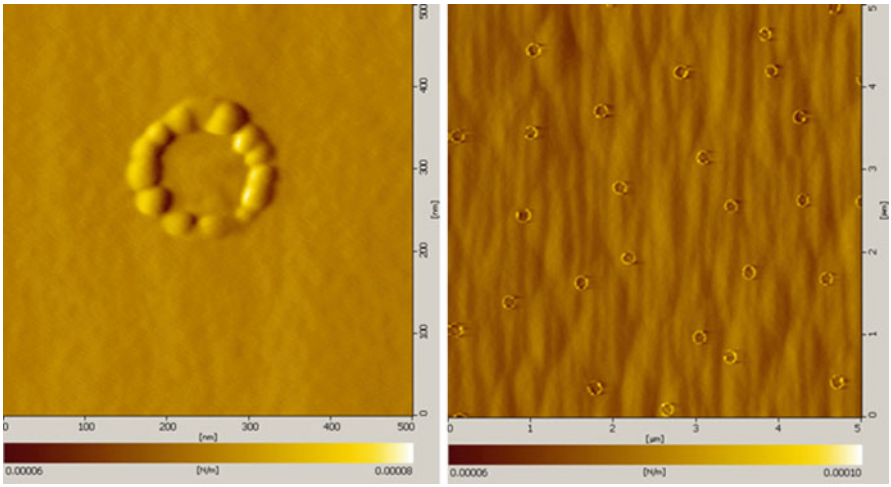

Fig. 2.6 AFM image of InP ring-shaped QDMs grown from In thickness 3.2 ML (crystallization temperature 200°C)

indium volume to each droplet spreading onto InGaP buffer layer. In this series of droplet epitaxy, the lowest indium thickness of 1.6 ML can provide only InP QR shape due to the limit volume of group III element. The ring robe is thin only around 1 nm, which does not give enough strain at InP/InGaP interface for QD formation. When thicker indium is deposited, QR becomes bigger in diameter. Strain is exhibited on the ring robe and then is relaxed by forming circular QD chain on the ring. QD uniformity is optimized at appropriate indium thickness. Further increase of indium thickness, QD size becomes larger and nonuniform.

Evolution of In droplets to InP ring-shaped QDMs by droplet epitaxy is shown step-wise in Fig. 2.8. The InP ring formation is originated from the crystallization at the outer peripheral of In droplets under P pressure together with the out diffusion of In atoms from the center of the droplets. At the same time, InP/InGaP lattice mismatch becomes critical when In thickness reaches a certain value. The strain relaxation happens at the ring robe and gives birth to circular QD chain formation on the ring.

Deposition temperature is a key parameter to control the ring diameter, dot size, and number of QDs on the ring robe. Deposition temperature is varied from 120 to 290°C for In deposition rate of 0.8 ML/s and In thickness of 3.6 ML. At a higher deposition temperature, a longer ring diameter, larger QD size, and larger number of QDs on the ring are obtained due to larger droplets being created by merging of small indium droplets. The density of InP ring-shaped QDMs is therefore decreased. The experimental results in this series of droplet epitaxy are displayed in Fig. 2.9. The uniformity of QD on the ring is optimized at a deposition temperature of 250°C. This value of deposition temperature is therefore widely used in other series of droplet epitaxy.

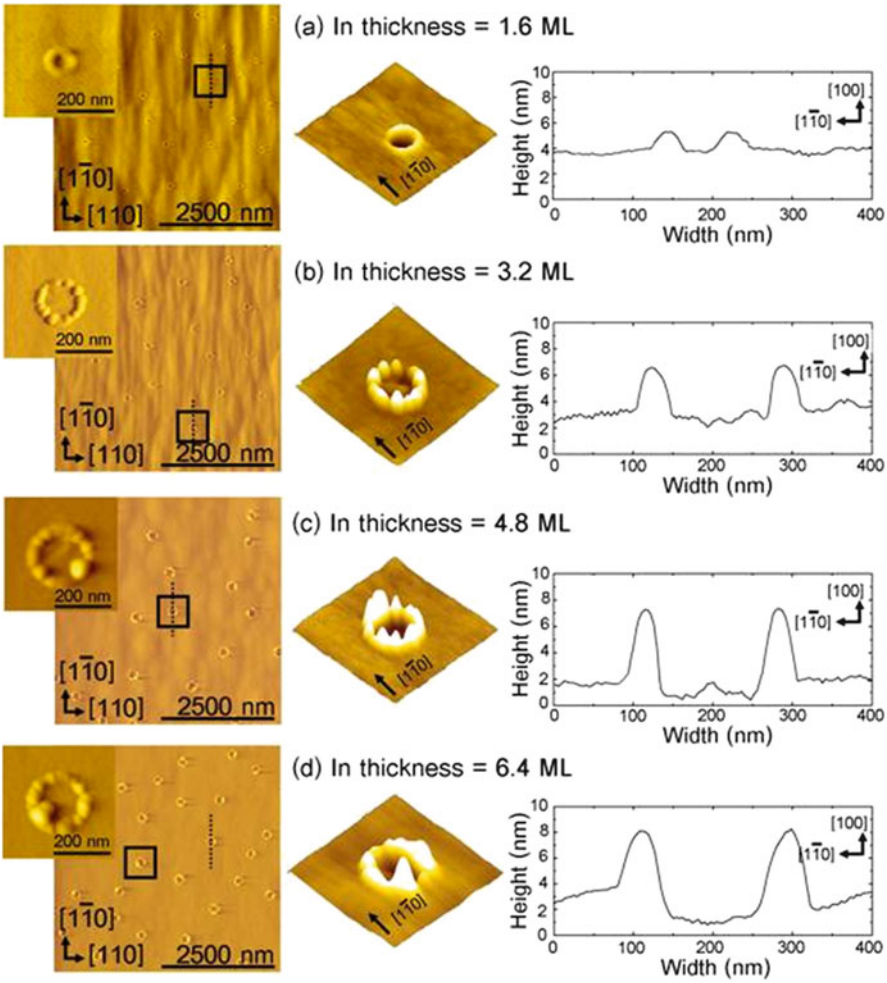

Fig. 2.7 In droplets are transformed to InP QRs and InP ring-shaped QDMs when more indium thickness is supplied from 1.6 to 6.4 ML during the deposition process. The deposition temperature and crystallization temperature are fixed at 250 and 200°C, respectively

When growth conditions at the deposition step are optimized and fixed like In thickness, In deposition rate and deposition temperature, in the next consecutive step of crystallization, InP ring-shaped QDMs will be affected by the crystallization temperature. At higher crystallization temperature, the ring diameter is longer but the QDM density and the number of QDs per QDM are smaller. Figure 2.10 shows the experimental results when crystallization temperature is varied from 150 to 300°C (deposition temperature 250°C, deposition rate 0.8 ML/s, indium thickness 3.2 ML). However, the effect of crystallization temperature on InP ring-shaped QDMs formation seems to be a secondary one. No large change in the nanostructure

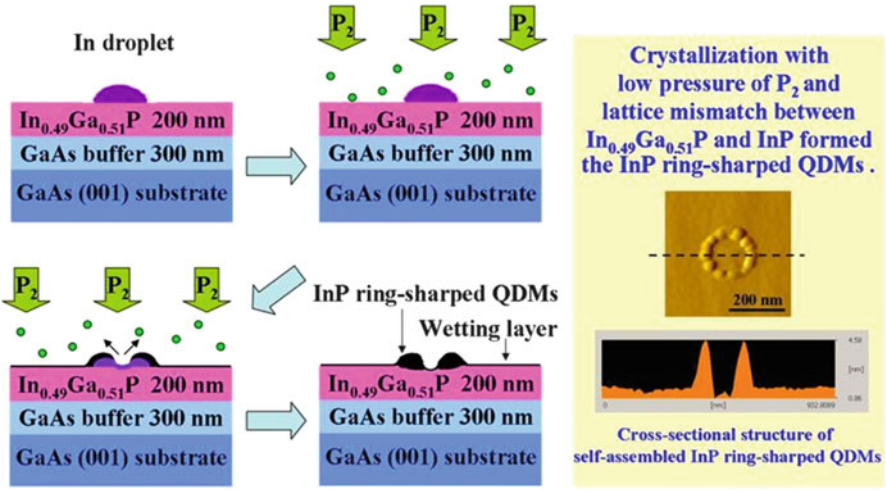

Fig. 2.8 Schematic displays of each processing steps of InP ring-shaped QDMs on InGaP/GaAs by droplet epitaxy technique

is observed, compared to the effect of primary step in the deposition process. Uniform QD is optimized at a crystallization temperature of 200°C.

In several series of experiments on droplet epitaxy, we can optimize the growth conditions to give fine InP ring-shaped QDMs by setting the deposition temperature and crystallization temperature at 250 and 200°C, respectively. The ring shape and density as well as the dot size are mainly defined by indium thickness during deposition step.

The number of QDs per QDM is another feature that is needed to be controlled for QD device applications. QDMs with eight QDs in ring shape are one of our aims in fabricating InP ring-shaped QDMs. This octa-quantum dot molecule will be a quantum dot set applicable for extended quantum dot cellular automata (EQCA). The concept of QCA will be discussed in detail in the following section.

When InP ring-shaped QDMs are capped by 100 nm thick InGaP for analytical photoluminescence measurement and for multi-stacked nanostructure, ring-shaped QDMs should be little affected by InP/InGaP matrix by using first InGaP capping layer grown by migration enhanced epitaxy technique at a low temperature of 300°C. To confirm the existence of ring-shaped QDMs, the sample is then prepared for TEM observation of their cross-sectional profiles. TEM image of InP ring-shaped QDMs grown at a deposition temperature of 250°C and a crystallization temperature of 200°C with indium deposition rate of 1.6 ML/s and indium thickness of 3.2 ML is shown in Fig. 2.11. TEM image can give actual dimensions of the nanostructure as follows. The outer and inner ring diameters are 140 and 80 nm, respectively. The basement of QD is approximately 40 nm with the dot height of few nm. These data are collected from the cross-sectional profile of the topmost nanostructure which has no thermal annealing effect by the capping process.

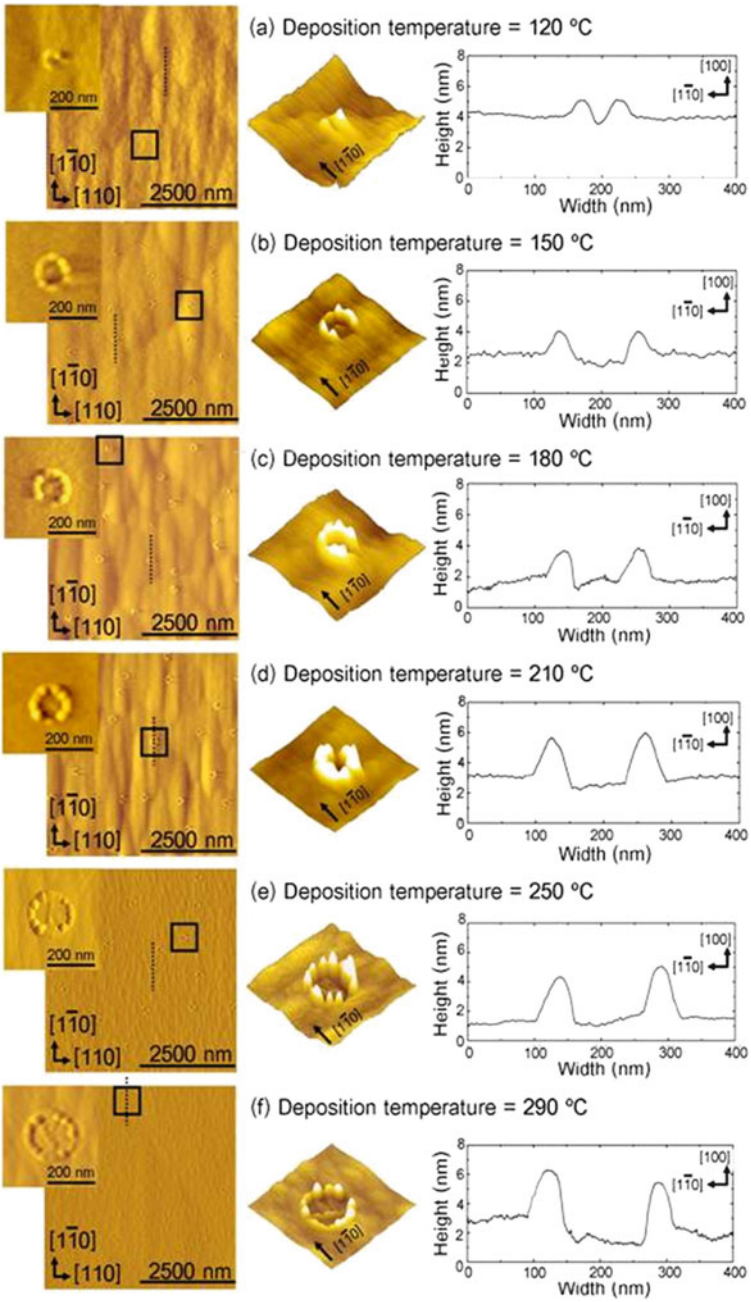

Fig. 2.9 When deposition temperature is varied from 120 to 290°C (crystallization temperature 200°C, In deposition rate 0.8 ML/s, In thickness 3.6 ML), InP ring-shaped QDMs become bigger in ring diameter, dot size, and number of dot on the ring with less QDM density due to merging of small droplets to larger droplet size leading to less droplet density at high deposition temperature

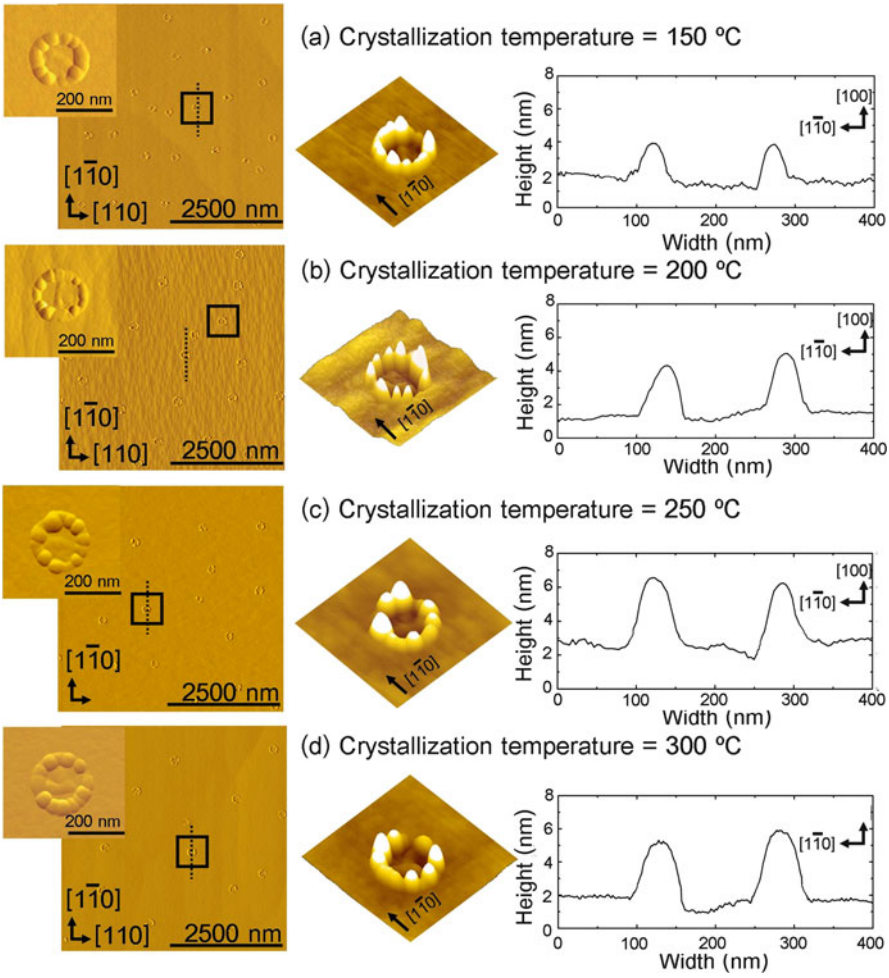

Fig. 2.10 InP ring-shaped QDMs being created at different crystallization temperatures from 150 to 300°C (In thickness 3.2 ML, In deposition rate 0.8 ML/s, and deposition temperature 250°C)

Capped samples of several InP ring-shaped nanostructures are also tested for their photoluminescence spectra. Their optical characteristics will be reported and discussed in the following section.

2.5 Photoluminescence Spectra of InP Ring-Shaped QDMs

InP is a direct bandgap (1.344 eV) semiconductor material. It gives strong light emission at a near infrared wavelength. When InP nanostructure is formed and is capped by a wider bandgap of InGaP, the emission wavelength is shifted to a shorter one in the red light region.

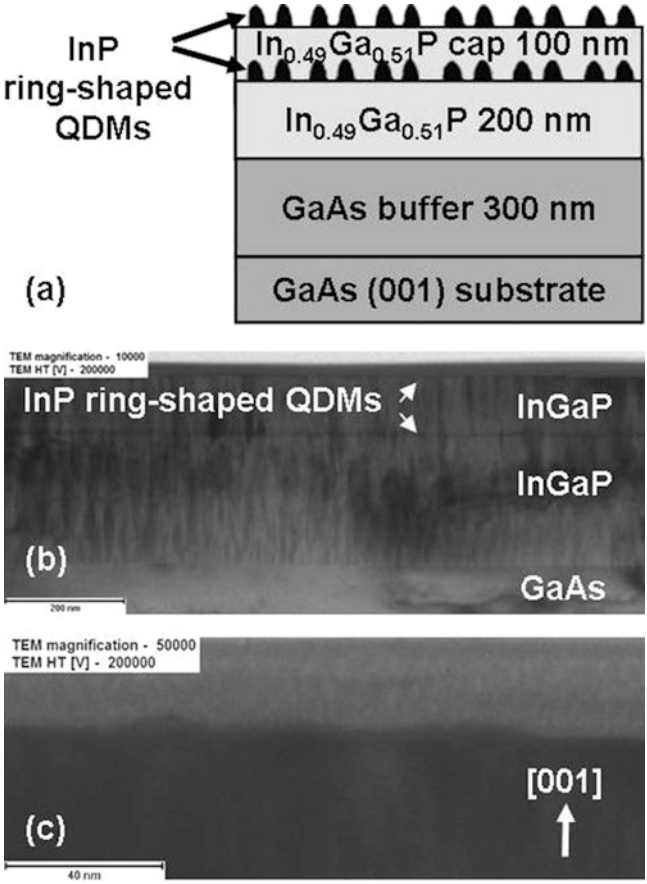

Fig. 2.11 TEM image of InP ring-shaped QDMs grown from In thickness 3.2 ML with deposition rate of 1.6 ML/s at a deposition temperature of 250°C and a crystallization temperature of 200°C

When InP ring-shaped QDMs are excited by blue laser, PL emission at red light will be detected.

We use Ar+ laser with a 478 nm wavelength and laser power up to 80 mW for our PL excitation. The sample is set up in a liquid Helium cryostat for cooling down to 20 K. PL signal is detected by either a CCD detector or a liquid nitrogen cooled InGaAs detector.

Photoluminescence (PL) is a basic analytical tool in studying the formation of InP ring-shaped QDMs throughout our whole experiment. InP ring-shaped QDMs are composed of QD chains on the ring robe. QDs on the ring are self-assembled. Therefore, they are not uniform in QD size. The difference in QD size leads to a broad PL spectrum. The PL spectroscopy is used to determine the homogeneity of the QDs on the ring as well as their crystal quality.

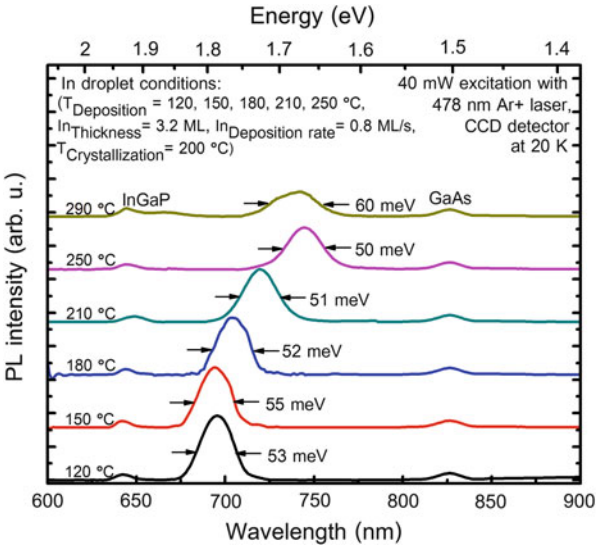

Fig. 2.12 PL spectra of InP ring-shaped QDMs with various deposition temperatures (120–290°C) excited by 40 mW Ar+ laser at 20 K

InP ring-shaped QDM samples grown with different deposition temperatures are investigated for their PL spectra. It is found that, at higher deposition temperatures, PL peaks are red-shifted due to a larger dot size. PL intensity becomes weakened due to lower QD density at a higher deposition temperature. FWHM is broader due to relaxed dot uniformity when deposition temperature is much higher than 250°C. (See details in Fig. 2.12.) This is a reason for fixing our deposition temperature at 250°C for the rest of our experiment.

At a fixed deposition temperature of 250°C, InP ring-shaped QDM samples are grown at different crystallization temperatures. Those samples are investigated for their PL spectroscopy. It is found from Fig. 2.13 that crystallization temperature is optimized at 200°C where PL peak becomes the highest and its FWHM is the narrowest.

From these two series of PL experiments, we find out that the deposition and crystallization temperatures have similar effects on the physical and optical properties of InP ring-shaped QDMs. The effect of deposition temperature is remarkably strong, since the QD and ring-shaped QDM sizes are determined during the deposition process prior to the following crystallization. We conclude that the deposition and crystallization temperatures are likely to be at 250 and 200°C, respectively. Under these conditions, PL peak is emitted at 750 nm with an FWHM of 50 meV at 20 K.

The next growth parameter to be investigated is In deposition rate. InP ring-shaped QDMs are grown at deposition and crystallization temperatures of 250 and 200°C with different In deposition rates (0.2–1.6 ML/s). Those samples are then evaluated for their PL spectroscopy as shown in Fig. 2.14.

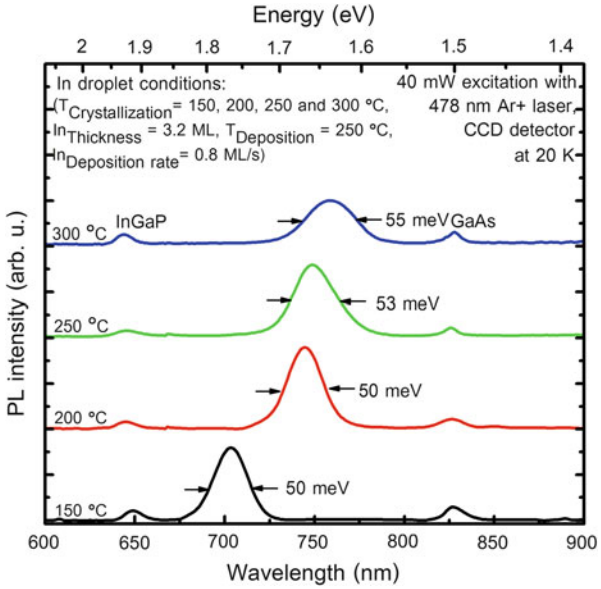

Fig. 2.13 PL spectra of InP ring-shaped QDMs with various crystallization temperatures (150–300°C) excited by 40 mW Ar+ laser at 20 K

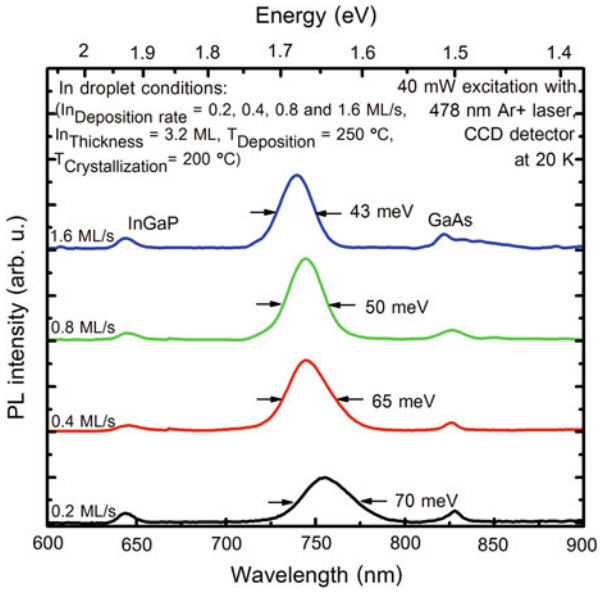

Fig. 2.14 PL spectra of InP ring-shaped QDMs with various indium deposition rates (0.2–1.6 ML/s) excited by 40 mW Ar+ laser at 20 K

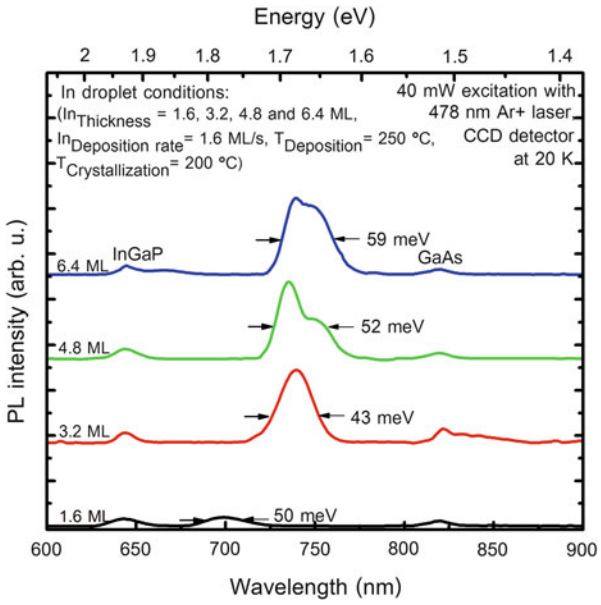

Fig. 2.15 PL spectra of InP QRs and InP ring-shaped QDMs with different indium thicknesses (1.6–6.4 ML) excited by 40 mW Ar+ laser at 20 K

It is found from this series of experiment that the higher indium deposition rate yields the better QD quality, and QD uniformity can be achieved. At 1.6 ML/s indium deposition rate, PL peak is blue-shifted to 740 nm wavelength with FWHM of 43 meV. We find also that, at this 1.6 ML/s deposition rate of indium, the percentage of creating octa-QDMs is as high as 46%. It is unfortunate that higher deposition rate than 1.6 ML/s could not be conducted due to the limitation of In cell temperature in our MBE equipment.

Final growth parameter to be optimized is indium thickness which gives more volume to the formation of InP ring-shaped QDMs. At a low indium thickness of 1.6 ML, only InP QRs are formed. Densities of QDs and of ring-shaped QDMs, number of QDs per ring-shaped QDMs and dimensions of QDs and of ring-shaped QDMs are increased with indium thickness greater than 1.6 ML. InP QRs and InP ring-shaped QDM samples with different indium thicknesses (1.6–6.4 ML) are evaluated for their crystal quality and homogeneity via PL measurement. At higher indium thickness than 3.2 ML, QDMs lose their dot uniformity. PL peak begins to split into two peaks because of the QD inhomogeneity attributed to two variations of QD height which can be confirmed from their respective AFM images. PL spectra have broader FWHM as shown in Fig. 2.15.

From the whole series of PL experiments, we optimize the growth conditions for InP ring-shaped QDM formation by droplet epitaxy as follows. The deposition

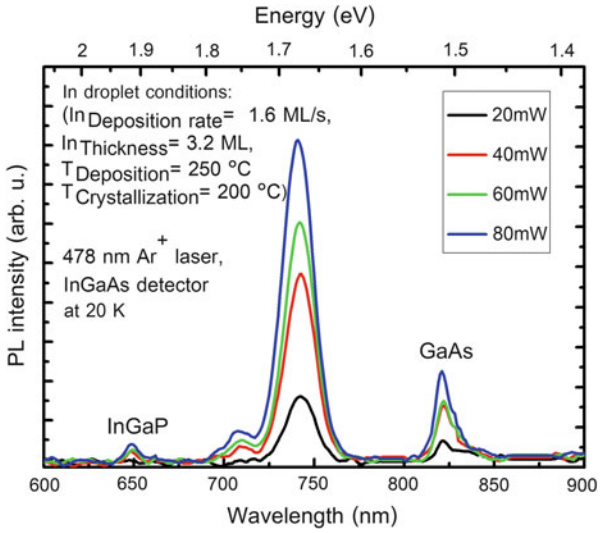

Fig. 2.16 Power dependence of PL emission from InP ring-shaped QDMs at 20 K

and crystallization temperatures are 250 and 200°C, respectively, with indium deposition rate of 1.6 ML/s and with indium thickness of 3.2 ML. Under these optimized growth conditions, the best QD size uniformity and the percentage of octa-QDMs as high as 46% can be maintained.

In order to understand the optical behavior of InP ring-shaped QDMs, further experiment on photoluminescence is continued by changing the excitation power and sample temperature. Figure 2.16 shows laser power dependence of PL emission from InP ring-shaped QDMs. The main PL peak is originated from the ground state having an emission wavelength of 740 nm, which is slightly blue-shifted at high excited laser power. PL peaks have FWHM values of 40–45 meV reflecting the uniformity of QDs on the rings. At high laser power, a weaker PL peak from the first excited state is also detected at 710 nm. In the PL spectra, PL emissions from InGaP and GaAs bulk materials are also observed at 650 and 850 nm, respectively.

When laser power excitation is fixed at 40 mW and sample temperature is varied from 20 to 100 K, temperature dependence of PL from InP ring-shaped QDMs is measured. The experimental result is shown in Fig. 2.17.

At a high sample temperature, PL peaks are red-shifted and FWHMs are broadened. PL signal is weakened due to thermal carrier escape from QDs to In0.5Ga0.5P capping layer. Defects in MEE grown In0.5Ga0.5P would trap those carriers leading to lower PL signal in a high temperature range.

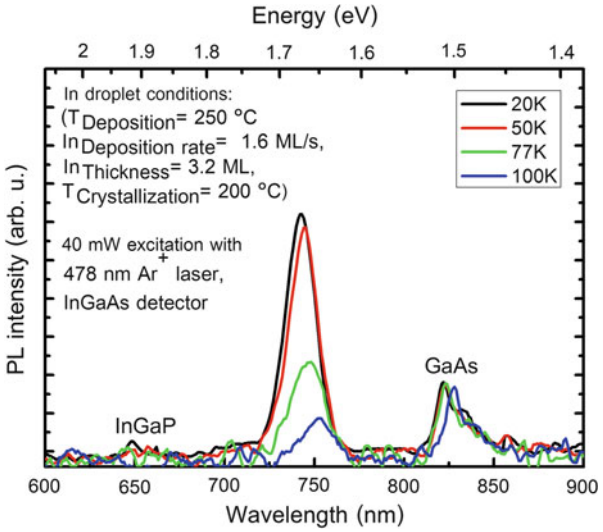

Fig. 2.17 Temperature dependence of PL emission from InP ring-shaped QDMs

2.6 Number of QDs per Ring and Potential Applications of InP Ring-Shaped QDMs

The growth parameters can modify QRs to ring-shaped QDMs. With limited volume of In thickness less than 1.6 ML, only QRs are realized. Increase in In deposition under appropriate crystallization condition with P pressure, InP QDs are created on the ring robe. The critical thickness for QD formation on the ring robe is in the range of 1.6–3.2 ML.

At a deposition temperature of 250°C and a crystallization temperature of 200°C, when In deposition rate of 1.6 ML/s and with In coverage of 3.2 ML, 46% of InP ring-shaped QDMs have eight dots per ring. These octa-QDMs are an interesting feature for extended quantum cellular automata application as shown in Fig. 2.18.

The basic idea of QCA is based on two electrons being located in quadra quantum dot set in diagonal positions due to Coulomb repulsion. The position of this electron pair can be either left or right diagonal configuration which represents either "1" or "0" in the binary system.

In octa QDMs having eight QDs per cell, the electron pair will have more stable positions, i.e., two diagonal configurations and more vertical and horizontal configurations. The EQCA gives more logic encodings as "1", "0", "+1/2," and "−1/2". This would enable QDMs to be utilized in future sophisticated quantum memory and computation.

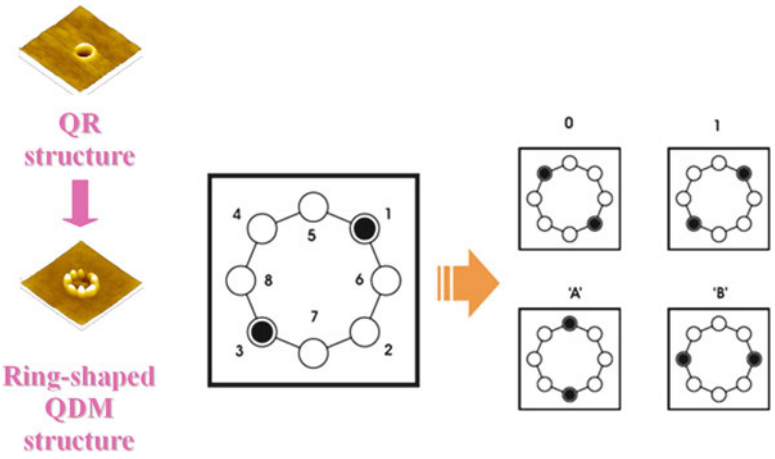

Fig. 2.18 Octa-QDMs can encode more logic values of 1, 0, and 1/2 for extended quantum dot cellular automata (EQCA) application

2.7 Summary

In this presentation, we intensively study the droplet epitaxial growth of InP ring-shaped QDMs. The quantum nanostructure is created on In0.5Ga0.5P/GaAs substrate based on the combination of droplet epitaxy technique for QR formation and strain-driven mechanism due to lattice mismatch between InP and In0.5Ga0.5P for QD formation on the ring robe when the critical thickness of indium coverage is reached.

Based on the AFM observation together with TEM confirmation and the experimental results on photoluminescence of the InP ring-shaped QDMs, we optimize the growth parameters as follows: the deposition and crystallization temperatures at 250 and 200°C with indium deposition rate of 1.6 ML/s and indium thickness of 3.2 ML. The QDMs with eight QDs per ring are our target in the fabrication which has a potential application in EQCA. The percentage of these ring-shaped octa-QDMs at the optimized growth condition is about 46%.

Acknowledgments This research article is an output which is supported by Thailand Research Fund (TRF) and Office of High Education Commission (OHEC) of Thailand in combined projects, i.e. Senior Research Scholar (RTA5080003), Distinguished Professor Grant (DPG5380002), the Royal Golden Jubilee Ph.D. program (Grant No. PHD/0040/2549). This research work is also supported by the Higher Education Research Promotion and National Research University Project of Thailand, Office of the Higher Education Commission (EN1180A-55) as well as by Nanotechnology Center of Thailand with counterpart fund from Chulalongkorn University.

References

1. Schmidt, O.G., Eberl, K.: Phys. Rev. B **61**, 13721 (2000)
2. Alfarov, Z.: Rev. Mod. Phys. **73**, 767 (2001)
3. Grundmann, M.: Physica E **5**, 167–184 (2000)
4. Tanabe, K., et al.: Appl. Phys. Lett. **100**, 193905 (2012)
5. Laouthaiwattana, K., et al.: Sol. Energy Mater. Sol. Cell **93**, 746–749 (2009)
6. Suraprapapich, S., et al.: J. Vac. Sci. Technol. B **24**, 1665 (2006)
7. Boonpeng, P., et al.: Microelectron. Eng. **86**, 853–856 (2009)
8. Wang, Z.M., et al.: Appl. Phys. Lett. **84**, 1931 (2004)
9. Lent, C.S., et al.: Nanotechnology **4**, 49–57 (1993)
10. Lent, C.S., Tougaw, P.D.: Proc. IEEE **85**, 491 (1997)
11. Porod, W.: J. Franklin Inst. **334B**(5/6), 1147–1175 (1997)
12. Bajec, I.L., et al.: Microelectron. Eng. **83**, 1826–1829 (2006)
13. Fisher, A.M.: Phys. Rev. Lett. **102**, 076405 (2009)
14. Watanabe, K., et al.: Jpn. J. Appl. Phys. **39**, 179–181 (2000)
15. Yamagiwa, M., et al.: Appl. Phys. Lett. **29**, 113115 (2006)
16. Sanguinetti, S., et al.: J. Appl. Phys. **104**, 113519 (2008)
17. Stemmann, A., et al.: J. Appl. Phys. **106**, 064315 (2009)
18. Mano, T., Mano, T., et al.: Thin Solid Films **515**, 531–534 (2006)
19. Heyn, C., et al.: Appl. Phys. Lett. **90**, 203105 (2007)
20. Strom, N.W., et al.: Nano Res. Lett. **2**, 112 (2007)
21. Esser, N., et al.: J. Vac. Sci. Technol. B **19**, 1756–1761 (2001)
22. Naraporn, P., et al.: J. Cryst. Growth **323**, 282–285 (2011)
23. Kurtenbach, A., et al.: J. Electron. Mater. **25**, 395–400 (1996)
24. Zundel, M.K., et al.: Appl. Phys. Lett. **73**, 1784–1786 (1998)
25. Lewis, G.M., et al.: Appl. Phys. Lett. **85**, 1904–1906 (2004)
26. Suraprapapich, S., et al.: Appl. Phys. Lett. **90**, 183112 (2003)
27. Suraprapapich, S., et al.: J. Cryst. Growth **302**, 735–739 (2007)
28. Mano, T., Kiguchi, N.: J. Cryst. Growth **278**, 108–112 (2005)
29. Lee, J.H., et al.: J. Appl. Phys. **106**, 073106 (2009)
30. Mazur, Y.I., et al.: Appl. Phys. Lett. **86**, 063102 (2005)
31. Somaschini, C., et al.: Nanotechnology **20**, 185602 (2011)

http://www.springer.com/978-1-4614-8129-4

Quantum Dot Molecules
Wu, J.; Wang, Z.M. (Eds.)
2014, XI, 377 p. 187 illus., 164 illus. in color., Hardcover
ISBN: 978-1-4614-8129-4